Supporting information

Anaerobic digestion alters copper and zinc speciation

Samuel Legros[1,2*], Clément Levard[3], Claire-Emmanuelle Marcato-Romain[4], Maritxu Guiresse[5], Emmanuel Doelsch[2]

1 CIRAD, UPR Recyclage et risque, 18524 Dakar, Senegal
2 CIRAD, UPR Recyclage et risque, F-34398 Montpellier, France
3 Université d'Aix-Marseille, CNRS, IRD, Collège de France, CEREGE, F- 13545 Aix en Provence, France
4 Université de Toulouse, UPS, LBAE (EA 4565), IUT 'A', 24 rue d'Embaqués, F-32000 Auch, France
5 EcoLab (Laboratoire d'Ecologie Fonctionnelle et Environnement), ENSAT, INP, UPS, Université de Toulouse, UMR CNRS 5245, F-31326 Castanet Tolosan, France

e-mail address: samuel.legros@cirad.fr

*Corresponding author. TEL : +221 33 849 33 17; Fax : +221 33 849 16 75

Number of pages: 14

Number of tables: 10

Number of figures: 9

Part SI-1: Complementary analysis in raw and digested wastes

Table SI-1: Complementary major element concentrations in raw and digested wastes

	Al		Na		Ca		Mg		K	
	R*	D	R	D	R	D	R	D	R	D
	g/kg	g/kg	g/kg	g/kg	g/kg	g/kg	g/kg	g/kg	g/kg	g/kg
PS	1.63	1.96	5.17	7.78	52.24	46.88	16.11	22.84	22.85	45.96
MWFF	14.31	24.14	8.97	10.03	47.41	73.53	5.68	7.76	9.15	13.61
SS	11.90	19.08	0.78	4.86	15.01	31.63	4.75	7.85	8.15	17.32
SSGW	10.59	17.77	0.82	2.38	14.94	27.06	4.52	8.22	10.27	21.49

*R = raw, D = digested

Table SI-2: Complementary trace element concentrations in raw and digested wastes

	Mn		Ti		Pb		Ni		Cr		Cd	
	R*	D	R	D	R	D	R	D	R	D	R	D
	mg/kg	mg/kg	mg/kg	mg/kg	mg/kg	mg/kg	mg/kg	mg/kg	mg/kg	mg/kg	mg/kg	mg/kg
PS	639	625	119	161	24.2	11.3	12.1	12.4	17.5	17.2	0.45	0.55
MWFF	187	266	1296	2260	66.0	95.2	122	54.6	278	124	0.86	0.57
SS	92.7	171	791	1349	59.1	80.6	29.7	38.7	59.4	93.0	1.43	2.29
SSGW	86.3	171	957	1464	40.2	66.8	20.9	35.4	50.4	84.3	1.30	2.53

*R = raw, D = digested

Part SI-2: Details concerning Zn and Cu K-edge EXAFS spectra data processing, PCA, TT and LCF

Zn and Cu species in the samples were determined using libraries of Zn and Cu model compounds. A methodology combining principal component analysis (PCA), target transformation (TT) and linear combination fitting (LCF) was used.

Principal component analysis (PCA) defines the minimum number of significant independent sources of variation. Those components, associated with a coefficient (eigenvalue), help explain the variance of the data matrix[1]. Principal component analysis was performed using SixPack software (Stanford, CA). For zinc, EXAFS $k^2\chi Zn(k)$ spectra were used in the 2.5 to 10.7 $Å^{-1}$ range, while for copper, EXAFS $k^2\chi Cu(k)$ spectra were used in the 2.5 to 10 $Å^{-1}$ range. Tables SI-3 and SI-4 present the PCA output parameters for Zn and Cu, respectively, including the component spectra and the variability explained by the component (Var) for the first four components. The indicator values (IND) are assumed to be minimal when the minimal number of components necessary to explain the data matrix (within the experimental error range) is reached[2, 3]. In this study, IND was minimum with three components for Zn and two components for Cu.

Table SI-3: PCA results for zinc

Compoments	Eigenvalue	Variance	Cumulative Variance	IND
1	21.7	0.659	0.659	0.0216
2	3.99	0.121	0.781	0.0189
3	2.83	0.085	0.867	0.0148
4	1.36	0.041	0.908	0.0153
5	0.93	0.028	0.936	0.0176
6	0.64	0.019	0.956	0.0234
7	0.53	0.016	0.972	0.0338
8	0.34	0.010	0.982	0.0707
9	0.30	0.009	0.991	0.2666
10	0.27	0.008	1.000	NA

Table SI-4: PCA results for copper

Compoments	Eigenvalue	Variance	Cumulative Variance	IND
1	16.0	0.675	0.675	0.0134
2	2.45	0.103	0.778	0.0119
3	1.43	0.060	0.838	0.0125
4	1.13	0.047	0.886	0.0132
5	0.69	0.029	0.915	0.0167
6	0.54	0.022	0.937	0.0239
7	0.48	0.020	0.958	0.0382
8	0.44	0.018	0.976	0.0709
9	0.34	0.014	0.991	0.2081
10	0.21	0.008	1.000	NA

The PCA outputs (components and eigenvalues) are strictly mathematical variables without any chemical meaning.

Target transformation (TT) allows explaining the structural variation in the set of unknown samples spectra by testing of chemical species used as standards. TT then redefines abstract components into chemically meaningful real matrices. In this study, database references were tested by TT. The SPOIL function was used to assess whether a given references was an acceptable target[2, 3] . This is a non-negative dimensionless number for which < 1.5 values are considered to be excellent: 1.5-3 good, 3-4.5 fair, 4.5-6 poor, and > 6 unacceptable. Tables SI-5 and SI-6 show the SPOIL values for all reference compounds for Zn and Cu, respectively. Among these reference compounds, only 16 reference compounds were selected for Zn and 10 for Cu, according to their acceptable SPOIL values.

Table SI-5. Reference compound database for Zn according to their SPOIL values for target transformation with four components

Reference compounds selected	SPOIL	Reference compounds not selected	SPOIL
nano-sphalerite	1.00	Zn hydroxide	4.62
Zn-histidine	2.02	kerolite	4.89
sphalerite	2.85	parahopeite	4.97
willemite	3.18	Zn-oxalate hydrate	5.04
Zn-citrate	3.34	Zn-LDH	5.07
Zn-cysteine	3.38	Zn-HIM	5.90
Zn-malic	3.54	Zn sulfate	8.32
apatite	3.67	ghanite	8.55
Zn-acetate dihydrate	3.75	zincite	11.5
Zn-phytate	3.97	franklinite	16.1
Zn-sorbed goethite	4.05		
Zn-methionine	4.05		
smithonite	4.09		
Zn-sorbed ferrihydrite	4.10		
Zn-metal	4.41		
Zn-nitrate	4.42		

Table SI-6: Reference compound database for Cu according to their SPOIL values for target transformation with four components

Reference compounds selected	SPOIL	Reference compounds not selected	SPOIL
Cu_I_Methionine	1.20	Cu_I_acetate	3.64
Cu_II_histidine	1.92	Cu_II adsorb_ferrihydrite	3.94
Cu_II_phtalocyanine	1.97	chalcopyrite	3.99
Cu_II_Malic	2.20	Cu sulfate	4.37
Cu_II_galacturonic	2.23	Cu_II_acetate	4.43
chalcocite	2.23	covellite	4.76
Cu_II_phenylalanine	2.68	Cu hydroxide	5.25
Cu_II_gluconate	2.89	malachite	5.83
Cu_I_thiophenolate	3.02	cornetite	6.68
Cu metal	3.07	cuprite	7.96
Cu_I_cysteine	3.18	tenorite	8.04

In complex matrices like organic wastes, the classical "shell by shell" fitting approach may be unsuitable because of the numerous second neighbor nature, distance, and number possibilities[3]. Alternatively, since the EXAFS spectrum of the unknown sample is a weighted sum of all species spectra present, the atomic fraction of each metal species can be obtained by **linear combination fits (LCF)** of this spectrum to reference spectra[4]. For the spectral reconstruction of our sample by LCF, we tested all three component combinations with these significant references. We also tested LCFs using successively two, three and four components. LCFs with n + 1 components were retained if the normalized sum-squares residual was decreased by more than 20% compared to the fit with n components 5 [5].

$$NSS = 100 \times \frac{\sum_{i=1}^{N}\left[k^2\chi(k_i)_{measured} - k^2\chi(k_i)_{fitted}\right]^2}{\sum_{i=1}^{N}\left[k^2\chi(k_i)_{measured}\right]^2} \quad (1)$$

N is the number of points, $k^2\chi(k_i)_{measured}$ is the EXAFS spectrum of the sample in the k-space and $k^2\chi(k_i)_{fitted}$ is the EXAFS fit in the K-space

These criteria enabled us to determine two or three significant components in all of the studied organic waste samples. Table SI-7 and SI-8 present the LCF results for Zn and Cu, respectively.

Table SI-7: proportion (%) of Zn reference compounds in each waste determined by the linear combination fits of Zn EXAFS

Sample name	References				NSS	Sum
	Zn phytate	Zn asorbed ferrihydrite	Nano-sphalerite	Zn histidine		
PS	39%	70%			2.35	109%
PS_D	93%	23%			3.38	112%
MWFF		83%	13%	13%	1.53	109%
MWFF_D		71%	28%	11%	1.55	109%
SS	54%	22%	25%		1.73	101%
SS_D	60%	13%	32%		1.89	104%
SSGW	62%	30%	7%		1.61	99%
SSGW_D	47%	12%	47%		2.23	106%

Table SI-8: proportion (%) for Cu reference compounds in each waste determined by linear combination fits of Cu EXAFS

	References				NSS	Sum
Sample Name	Cu(II)phtalocyanine	Cu(II)histidine	Cu(II)galacturonic	Cu(I)methionine		
PS		45%	36%	15%	4.40	96%
PS_D		78%		23%	3.60	100%
MWFF	29%		36%	27%	2.79	92%
MWFF_D	18%		33%	49%	3.55	99%
SSGW		28%	27%	39%	2.00	94%
SSGW_D			44%	46%	2.58	90%
SS			56%	34%	4.36	89%
SS_D			50%	54%	4.09	103%

Part SI-3 Reference compound database for XAS

Table SI-9: Reference compound database for Zn

Reference compounds [Formula]	Neighbors atoms (symetry)	Bibliographic reference
nano-sphalerite [ZnS]	4 S @ 2.34 Å	[6]
Zn-histidine [Zn(C6H9N3O2)2]	4 N @ 2.02-2.04 Å	[7]
sphalerite [ZnS]	4 S @ 2.34 Å; 12 Zn @ 3.83; 12 S @ 4.49	[8]
willemite [Zn2SiO4]	4O @ 1.91-1.98 Å; 4 Zn @ 3.09-3.24 Å; 4Si @ 3.11-3.32 Å	[8]
Zn-citrate [Zn(C2H3O2)2.2H2O]	6O @ 2.03-2.29 Å	[9]
Zn-cysteine [Zn(C3H7NO2S)4]	4S @ 2.34 Å; 3C @ 3.29 Å	[10]
Zn-malic [Zn(C4H6O5)2]	4.2 O @ 2.01 Å; 1.9 C @ 2.8 Å	[10]
apatite	5.3O @ 1.98 Å; 1.6P @ 3.15 Å; 1.5Zn @ 3.36 Å	[11]
Zn Acetate [Zn(C2H3O2)2.2H2O]	6 O @ 2.12-2.18 Å	[7]
Zn_Phytate [Zn(C6H8(PO4)6)]	3.9O @ 1.96 Å; 1P @ 3.08 Å	[10]
Zn-sorbed goethite [Zn-(FeO)2]	6O @ 2.07-2.15 Å	[12]
Zn-Methionine [Zn(C5H11NO2S)2]	2N/O @ 2.03 Å; 2S @ 2.31 Å	[13]
smithonite [ZnCO3]	6O @ 2.10 Å; 6C @ 2.99; 6O @ 3.19; 6n@3.66	[11]
Zn-sorbed-fhyd [Zn-(FeO)2]	4O @ 1.93-2.0 Å	[12]
Zn-metal [Zn]	12 Zn @ 2.66 Å; 6 Zn @ 2.91; 6 Zn @ 3.95	[8]
Zn-nitrate [Zn(NO3)2]	6O @2.09 Å	[14]
Zn hydroxide [Zn(OH)2]	4O @ 1.95-1.97 Å	[8]
kerolite [Si4Zn3O10(OH)2]	5.4O @ 2.07 Å; 6Zn @ 3.11 Å; 4.7; Si @ 3.30 Å	[15]
parahopeite [Zn3(PO4)2.4H2O]	Site 1: 6O @ 2.10 Å; Site 2: 4O @ 1.92-2.00 Å	[16]
Zn Oxalate [Zn(C2H2O4)2.H2O]	4O + 2O from H_2O	[17]
Zn_LDH [Zn1-xAlx (OH)2]x	5 O @ 2.07 Å; 3.9 Zn @ 3.12 Å	[15]
Zn-HIM	5.7 O @ 2.05 Å; 3.8 Al @ 3.05 Å	[4]
Zn sulfate [ZnSO4.H2O]	5.6 O @ 2.07 Å;	[4]
ghanite [ZnAl2O4]	4.4O @ 1.97 Å; 14.5Al @ 3.41 Å	[4]
zincite [ZnO]	4O @ 1.96 Å; 12Zn @ 3.22 Å	[11]
franklinite [ZnFeO4]	4O @1.96 Å; 12Fe @ 3.51 Å	[4]

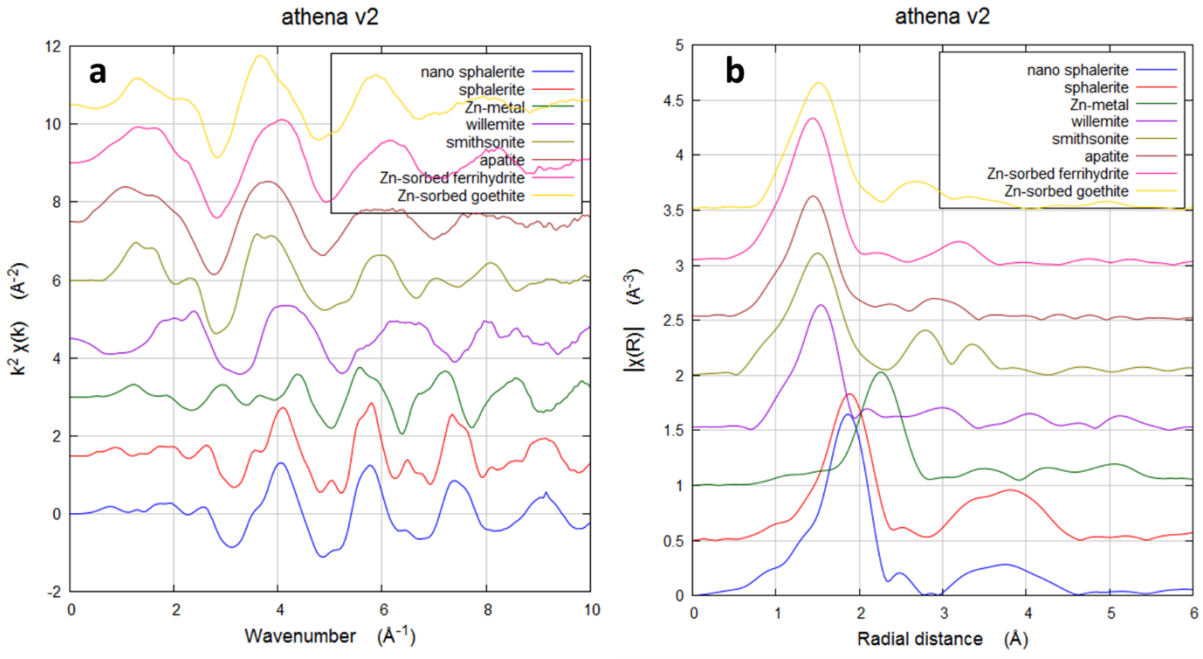

Figure SI-1: a) Zn $k^2\chi(k)$ EXAFS spectra selected inorganic zinc references and b) their respective radial distribution functions.

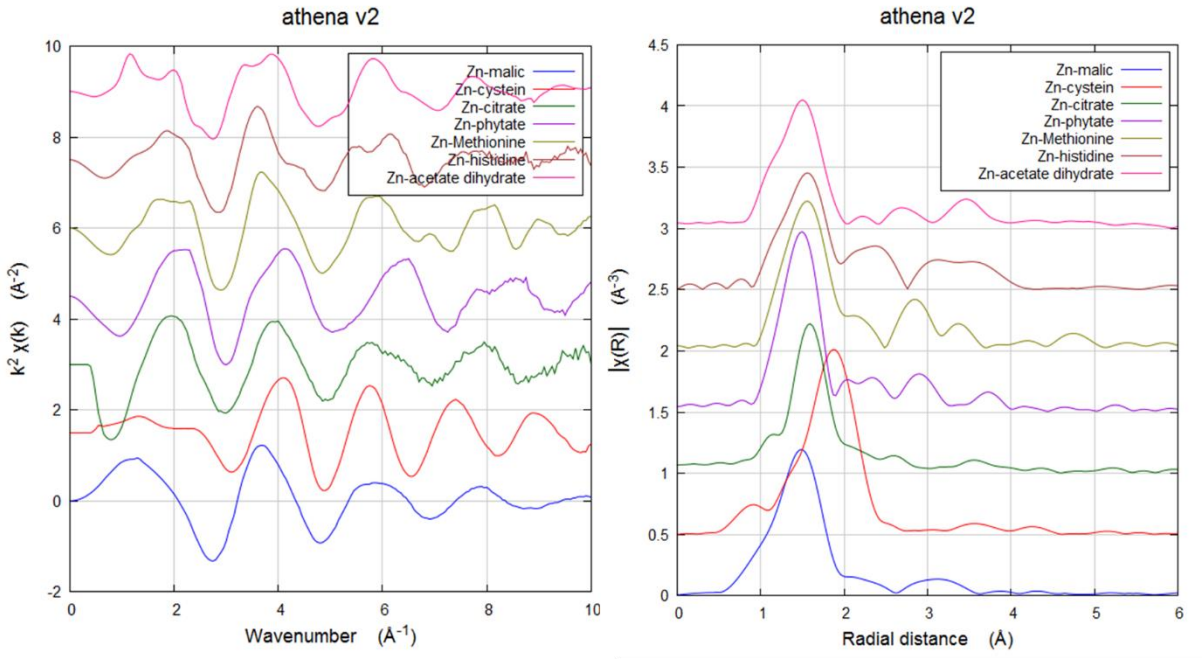

Figure SI-2: a) Zn $k^2\chi(k)$ EXAFS spectra selected organic zinc references and b) their respective radial distribution functions.

Table SI-10: Reference compound database for Cu

Reference compounds [Formula]	Oxidation state	Neighbor atoms (Symmetry)	Bibliographic reference
Cu-Methionine	Cu(I)	3 S (trigonal)	18
Cu-histidine	Cu(II)	4 O/N (Sq. planar)	19
Cu-phtalocyanine	Cu(II)	4 N (Sq planar)	20
Cu-Malic	Cu(II)	5/6-O-ring	21
Cu-galacturonic	Cu(II)	6 O (Dist. Oh)	22
chalcocite [Cu2S]	Cu(I)	3 S (trigonal) and 2 S (linear)	23
Cu-phenylalanine	Cu(II)	4 O (tetragonal)	24
Cu-gluconate	Cu(II)	4 O (Sq. planar)	25
Cu-thiophenolate [Cu(C6H5S)]	Cu(II)	3 S (trigonal)	26
Cu Metal [Cu]	Cu(0)	12 Cu	27
Cu-cysteine [Cu(C3H7O2SN)]	Cu(I)	3 S (trigonal)	28
Cu-acetate [Cu(C2H3O2)]	Cu(I)	2.5 O	25
Cu sorb Ferrihydrite [(≡FeO)3-Cu]	Cu(II)	6 O (dist. Oh)	29
chalcopyrite [CuFeS2]	Cu(II)	4 S (Td)	30
Cu sulfate [CuSO4 5H20]	Cu(II)	6 O (Dist. Oh)	27
Cu-acetate [Cu(C2H3O2)2]	Cu(II)	5 O	31
covellite [CuS]	Cu(II)	4 S (Td) and 3 S (trigonal)	23
Cu hydroxide [Cu(OH)2]	Cu(II)	6 O (Dist. Oh)	32
malachite [CuCO3]	Cu(II)	6 O (Dist. Oh)	33
cornetite [Cu3PO4OH3]	Cu(II)	6 O (Dist. Oh)	34
cuprite [Cu2O]	Cu(I)	2 O (linear)	35
tenorite [CuO]	Cu(II)	4 O (Sq planar)	27

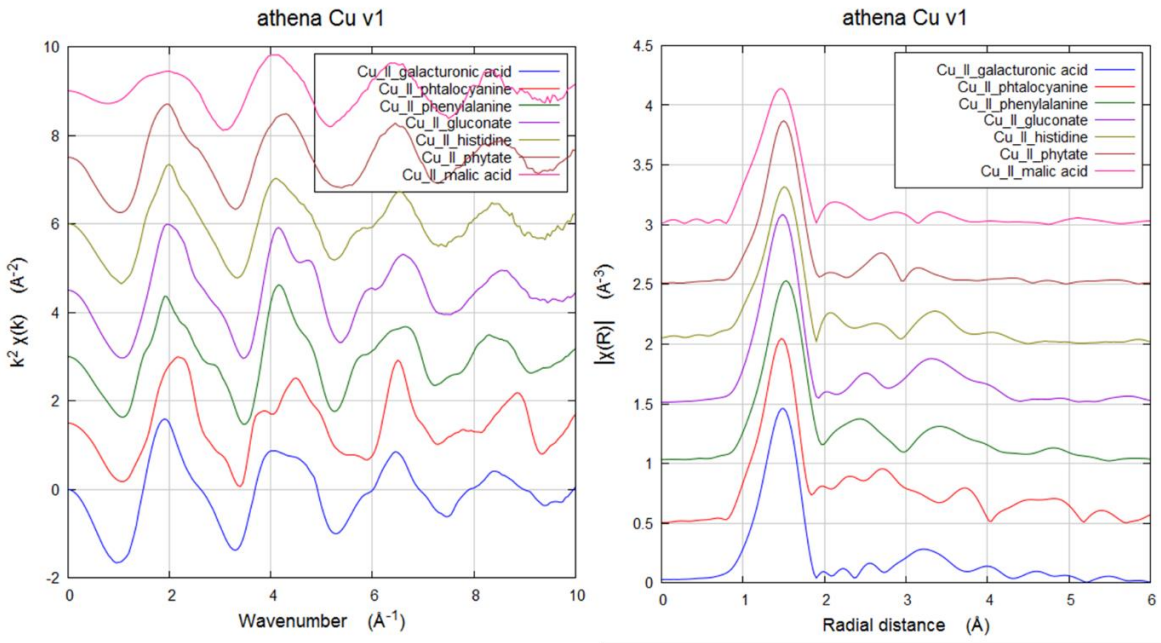

Figure SI-3: a) Cu $k^2\chi(k)$ EXAFS spectra of the selected Cu references with an oxidation state of 2 and b) their respective radial distribution functions.

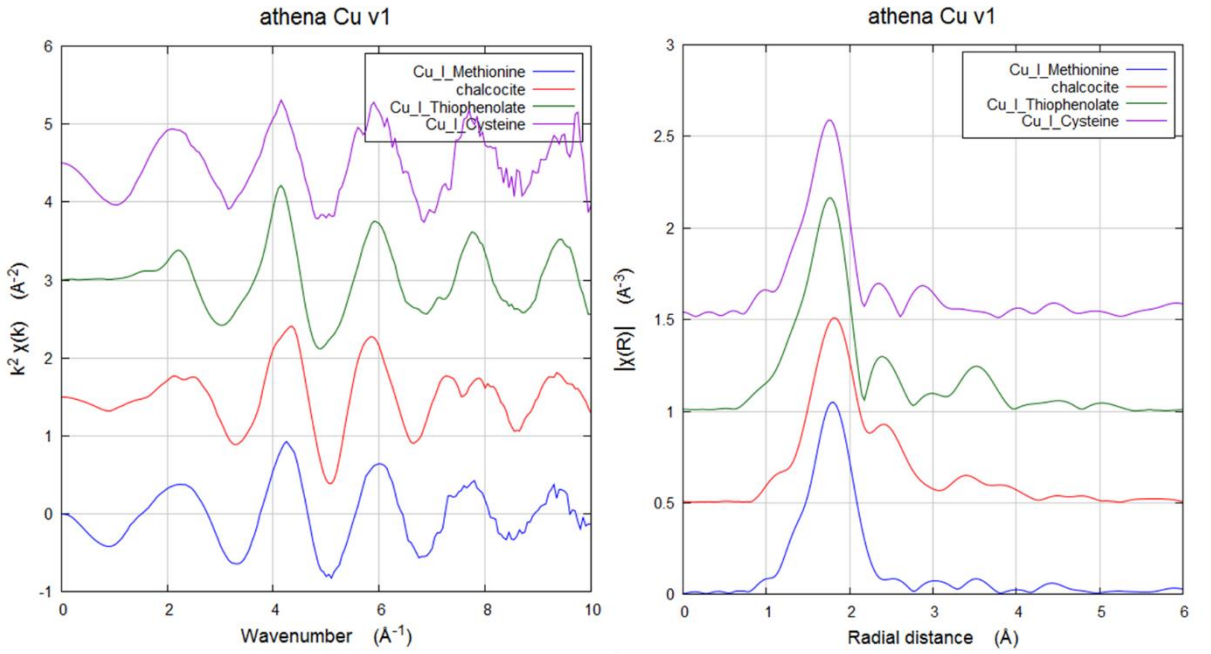

Figure SI-4: a) Cu $k^2\chi(k)$ EXAFS spectra of the selected Cu references with an oxidation state of 1 and b) their respective radial distribution functions.

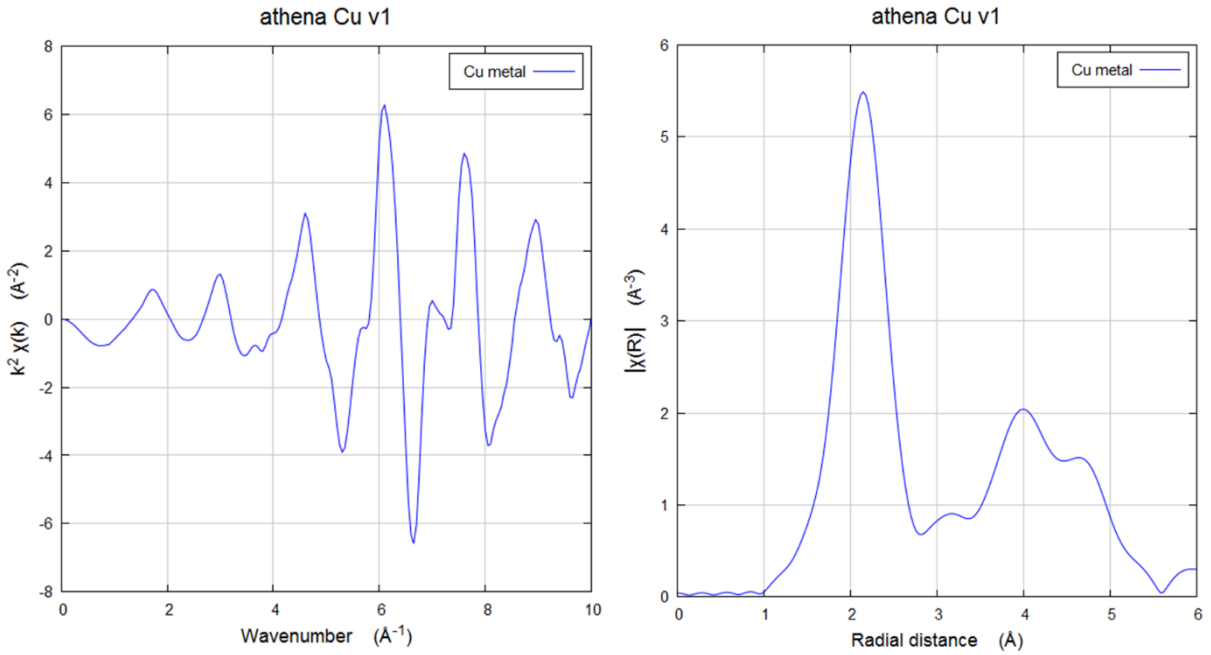

Figure SI-5: a) Cu $k^2\chi(k)$ EXAFS spectra of the selected Cu metal reference and b) its respective radial distribution functions.

Part SI-4: Comparison of EXAFS spectra of crystalline sulphides and organic or amorphous sulphides

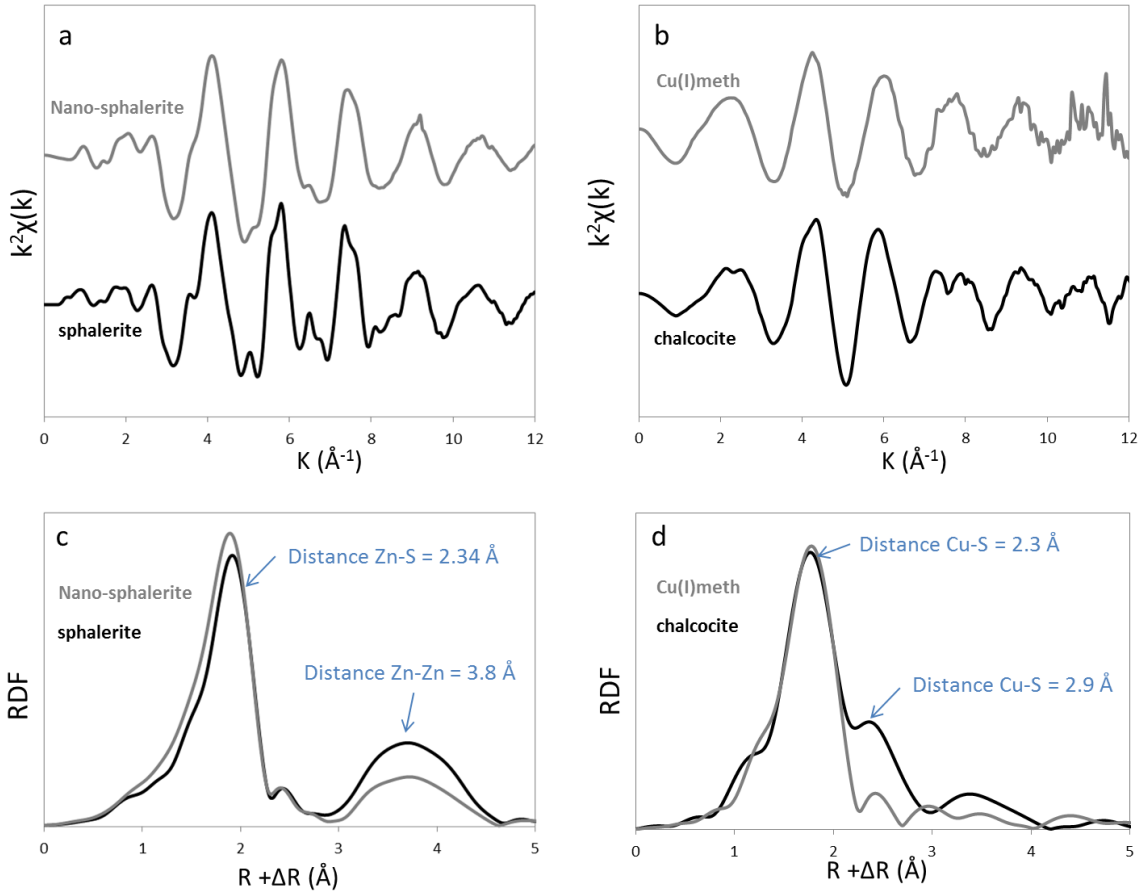

Figure SI-6: Comparison of $k^2\chi(k)$ EXAFS spectra of crystalline sulfides and organic or amorphous sulfides for a) zinc and b) copper and their respective radial distribution functions c) zinc and d) copper.

The EXAFS spectrum of nano-sphalerite (i.e sphalerite of around 3 nm in size) differs from that of bulk sphalerite (Figure SI-1a), specifically regarding the oscillations at 3.5, 5, 6.45 and 8.05 $Å^{-1}$ that are more pronounced in the EXAFS spectrum of bulk sphalerite. The first coordination shell is the same in both cases, with four S atoms at 2.34 Å[6, 36]. However, the second coordination shell is different, i.e. in the bulk sphalerite there are 12 Zn atoms at 3.83 Å, while in nano-sphalerite there are only 6 Zn atoms at 3.83 Å[6, 36]. This difference is visible in the radial distribution function (Figure SI-1c) where the second peak representing the Zn-Zn distance is lower for nano-sphalerite. Sphalerite nanoparticules exhibit a high fraction of under-coordinated surface atoms. Hence, the average Zn neigbouring atoms in the second coordination shell for nano-sphalerite is lower than for bulk sphalerite, leading to a less structured EXAFS spectrum.

The EXAFS spectra of Cu(I)methionine and chalcocite are quite similar (Figure SI-1b). In the two references, the first coordination shell presents S atoms at around 2.29 Å[18, 23, 26]. The EXAFS spectrum of chalcocite presents a second peak (Figure SI-1d) that could be interpreted as indicating the presence of S atoms at 2.90 Å[23]. Note that this peak was not observed with Cu(I)methionine (Figure SI-1d).

Part SI-5: Complementary XAS information for samples

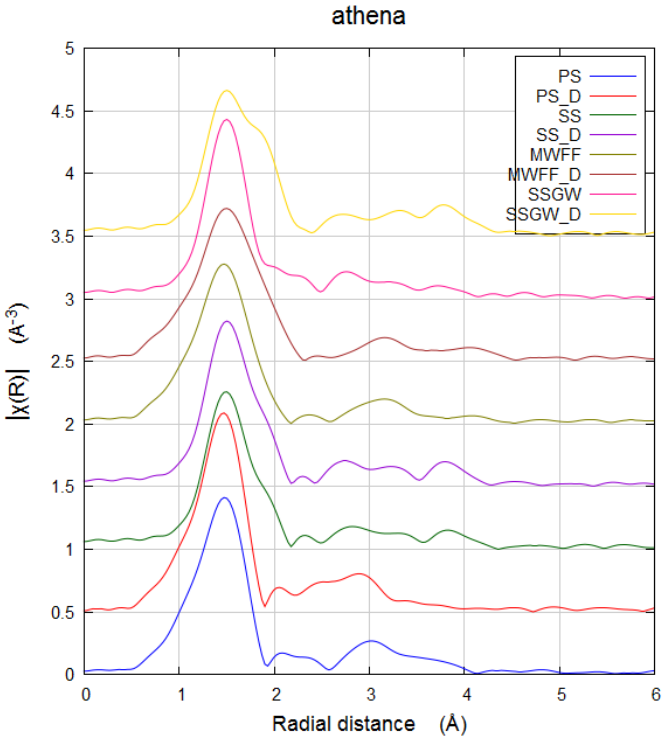

Figure SI-7: Radial distribution functions for all studied samples at Zn k edge.

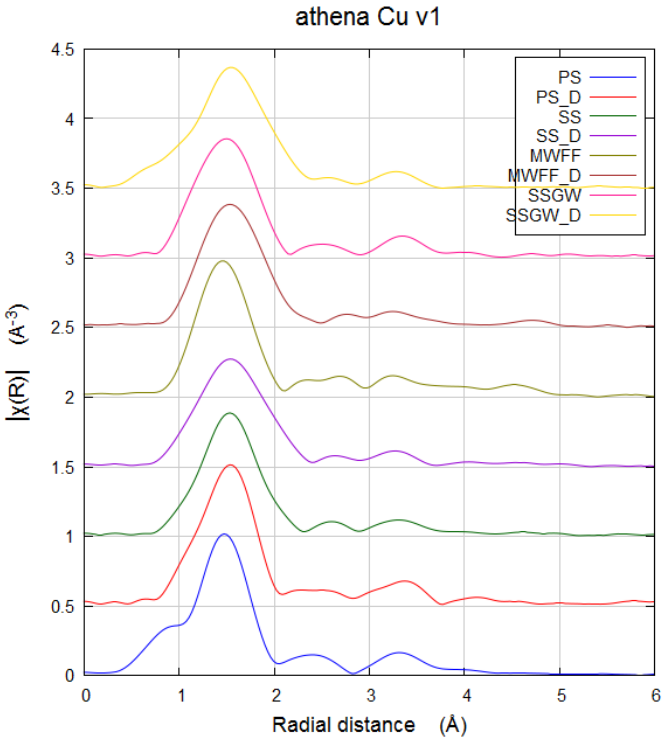

Figure SI-8: Radial distribution functions for all studied samples at Cu k edge.

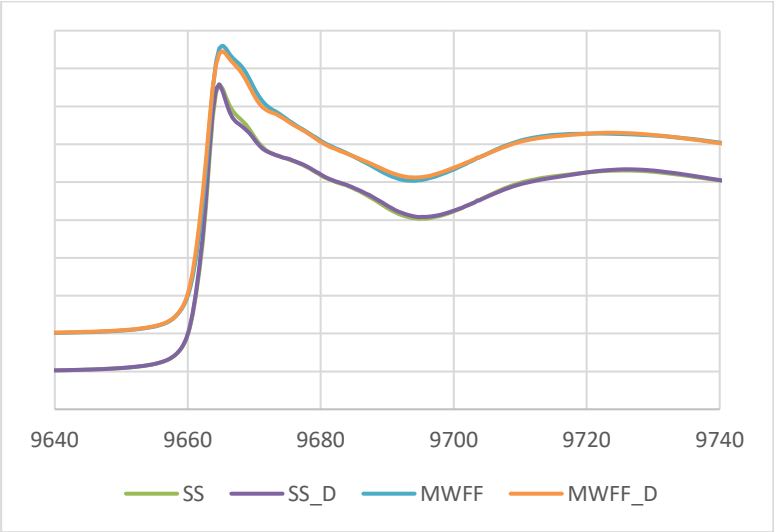

Figure SI-9: Zn XANES for SS and MWFF and their digested counterparts

Figure SI-4 shows that the Zn XANES is very similar for the studied samples. Therefore, it has not been used to perform the LCF.

References

1. Beauchemin, S.; Hesterberg, D.; Beauchemin, M. Principal Component Analysis Approach for Modelling Sulfur K-XANES Spectra of Humic Acids. *Soil Sci. Soc. Am. J.* **2002,** *66*, (1), 83-91.
2. Malinowski, E. R. Determination of the number of factors and the experimental error in a data matrix. *Anal. Chem.* **1977,** *49*, 612-617.
3. Manceau, A.; Marcus, M. A.; Tamura, N. Quantitative Speciation of Heavy Metals in Soils and Sediments by Synchrotron X-ray Techniques. *Rev. Minreal. Geochem.* **2002,** *49*, 341-428.
4. Scheinost, A. C.; Kretzschmar, R.; Pfister, S.; Roberts, D. R. Combining Selective Sequential Extractions, X-ray Absorption Spectroscopy, and Principal Component Analysis for Quantitative Zinc Speciation in Soil. *Environ. Sci. Technol.* **2002,** *36*, (23), 5021-5028.
5. Doelsch, E.; Basile-Doelsch, I.; Rose, J.; Masion, A.; Borschneck, D.; Saint Macary, H.; Bottero, J. Y. New Combination of EXAFS Spectroscopy and Density Fractionation for the Speciation of Chromium within an Andosol. *Environ. Sci. Technol.* **2006,** *40*, (24), 7602-7608.
6. Kim, B.; Levard, C.; Murayama, M.; Brown, G. E.; Hochella, M. F. Integrated Approaches of X-Ray Absorption Spectroscopic and Electron Microscopic Techniques on Zinc Speciation and Characterization in a Final Sewage Sludge Product. *J. Environ. Qual.* **2014,** *43*, (3), 908-916.
7. Sarret, G.; Manceau, A.; Spadini, L.; Roux, J.-C.; Hazemann, J.-L.; Soldo, Y.; Eybert-BÉrard, L.; Menthonnex, J.-J. Structural Determination of Zn and Pb Binding Sites in Penicillium chrysogenum Cell Walls by EXAFS Spectroscopy. *Environ. Sci. Technol.* **1998,** *32*, (11), 1648-1655.
8. Legros, S.; Chaurand, P.; Rose, J.; Masion, A.; Briois, V.; Ferrasse, J. H.; MacAry, H. S.; Bottero, J. Y.; Doelsch, E. Investigation of copper speciation in pig slurry by a multitechnique approach. *Environ. Sci. Technol.* **2010,** *44*, (18), 6926-6932.
9. Deng, Y.-F.; Zhou, Z.-H. Synthesis and crystal structure of a zinc citrate complex [Zn(H2cit)(H2O)] n. *J. Coord. Chem.* **2009,** *62*, (9), 1484-1491.

10. Sarret, G.; Saumitou-Laprade, P.; Bert, V.; Proux, O.; Hazemann, J. L.; Traverse, A.; Marcus, M. A.; Manceau, A. Forms of zinc accumulated in the hyperaccumulator Arabidopsis halleri. *Plant Physiol.* **2002,** *130*, (4), 1815-1826.
11. Lee, Y. J.; Elzinga, E. J.; Reeder, R. J. Sorption Mechanisms of Zinc on Hydroxyapatite: Systematic Uptake Studies and EXAFS Spectroscopy Analysis. *Environ. Sci. Technol.* **2005,** *39*, (11), 4042-4048.
12. Juillot, F.; Maréchal, C.; Ponthieu, M.; Cacaly, S.; Morin, G.; Benedetti, M.; Hazemann, J. L.; Proux, O.; Guyot, F. Zn isotopic fractionation caused by sorption on goethite and 2-Lines ferrihydrite. *Geochim. Cosmochim. Ac.* **2008,** *72*, (19), 4886-4900.
13. González, J. C.; Peariso, K.; Penner-Hahn, J. E.; Matthews, R. G. Cobalamin-Independent Methionine Synthase from Escherichia coli: A Zinc Metalloenzyme. *Biochemistry* **1996,** *35*, (38), 12228-12234.
14. Pokrovsky, O. S.; Viers, J.; Freydier, R. Zinc stable isotope fractionation during its adsorption on oxides and hydroxides. *J. Colloid. Interf. Sci.* **2005,** *291*, (1), 192-200.
15. Jacquat, O.; Voegelin, A.; Villard, A.; Marcus, M. A.; Kretzschmar, R. Formation of Zn-rich phyllosilicate, Zn-layered double hydroxide and hydrozincite in contaminated calcareous soils. *Geochim. Cosmochim. Ac.* **2008,** *72*, (20), 5037-5054.
16. Ghao, G. Y. Refinement of the crystal structure of parahopeite. *Z. Kristallogr.* **1969,** *130*, 161-266.
17. Sarret, G.; Balesdent, J.; Bouziri, L.; Garnier, J. M.; Marcus, M. A.; Geoffroy, N.; Panfili, F.; Manceau, A. Zn Speciation in the Organic Horizon of a Contaminated Soil by Micro-X-ray Fluorescence, Micro- and Powder-EXAFS Spectroscopy, and Isotopic Dilution. *Environ. Sci. Technol.* **2004,** *38*, (10), 2792-2801.
18. D'Angelo, P.; Pacello, F.; Mancini, G.; Proux, O.; Hazemann, J. L.; Desideri, A.; Battistoni, A. X-ray Absorption Investigation of a Unique Protein Domain Able To Bind both Copper(I) and Copper(II) at Adjacent Sites of the N-Terminus of Haemophilus ducreyi Cu,Zn Superoxide Dismutase†. **2005,** *44*, (39), 13144-13150.
19. Mesu, J. G.; Visser, T.; Soulimani, F.; van Faassen, E. E.; de Peinder, P.; Beale, A. M.; Weckhuysen, B. M. New Insights into the Coordination Chemistry and Molecular Structure of Copper(II) Histidine Complexes in Aqueous Solutions. *Inorg. Chem.* **2006,** *45*, (5), 1960-1971.
20. Gardea-Torresdey, J. L.; Peralta-Videa, J. R.; de la Rosa, G.; Parsons, J. G. Phytoremediation of heavy metals and study of the metal coordination by X-ray absorption spectroscopy. *Coordin. Chem. Rev.* **2005,** *249*, (17–18), 1797-1810.
21. Phillips, C. L.; Regier, T. Z.; Peak, D. Aqueous Cu(II)–Organic Complexation Studied in Situ Using Soft X-ray and Vibrational Spectroscopies. *Environ. Sci. Technol.* **2013,** *47*, (24), 14290-14297.
22. Synytsya, A.; Urbanová, M.; Setnička, V.; Tkadlecová, M.; Havlíček, J.; Raich, I.; Matějka, P.; Synytsya, A.; Čopíková, J.; Volka, K. The complexation of metal cations by d-galacturonic acid: a spectroscopic study. *Carbohyd. Res.* **2004,** *339*, (14), 2391-2405.
23. Pattrick, R. A. D.; Mosselmans, J. F. W.; Charnock, J. M.; England, K. E. R.; Helz, G. R.; Garner, C. D.; Vaughan, D. J. The structure of amorphous copper sulfide precipitates: An X-ray absorption study. *Geochim. Cosmochim. Ac.* **1997,** *61*, (10), 2023-2036.
24. Ganesan, A.; Dreyer, J.; Wang, F.; Akola, J.; Larrucea, J. Density functional study of Cu2+-phenylalanine complex under micro-solvation environment. *J. Mol. Graphics Model.* **2013,** *45*, 180-191.
25. Parsons, J. G.; Hejazi, M.; Tiemann, K. J.; Henning, J.; Gardea-Torresdey, J. L. An XAS study of the binding of copper(II), zinc(II), chromium(III) and chromium(VI) to hops biomass. *Michrochem. J.* **2002,** *71*, (2–3), 211-219.
26. Weininger, M. S.; Hunt, G. W.; Amma, E. L. Crystal and molecular structure of tris(ethylenethiourea)copper(I) sulphate and tris(tetramethylthiourea)copper(I) tetrafluoroborate [examples of trigonal planar copper(I) stereochemistry]. *J. Chem. Soc. Chem. Comm.* **1972**, (20), 1140-1141.

27. Lassesson, H.; Steenari, B.-M. Speciation of Copper in Ash from a Fluidized-Bed Boiler Fired with Municipal Solid Waste. *Energ. Fuel.* **2013,** *27*, (7), 3891-3897.
28. Jullien, A.-S.; Gateau, C.; Kieffer, I.; Testemale, D.; Delangle, P. X-ray Absorption Spectroscopy Proves the Trigonal-Planar Sulfur-Only Coordination of Copper(I) with High-Affinity Tripodal Pseudopeptides. *Inorg. Chem.* **2013,** *52*, (17), 9954-9961.
29. Scheinost, A. C.; Abend, S.; Pandya, K. I.; Sparks, D. L. Kinetic Controls on Cu and Pb Sorption by Ferrihydrite. *Environ. Sci. Technol.* **2001,** *35*, (6), 1090-1096.
30. Hall, S. R.; Stewart, J. M. The crystal structure refinement of chalcopyrite, CuFeS2. *Acta Crystallogr. B* **1973,** *29*, 579-585.
31. Sahi, S. V.; Israr, M.; Srivastava, A. K.; Gardea-Torresdey, J. L.; Parsons, J. G. Accumulation, speciation and cellular localization of copper in Sesbania drummondii. *Chemosphere* **2007,** *67*, (11), 2257-2266.
32. Oswald, H. R.; Reller, A.; W., S. H.; E., D. Structure of copper(II) hydroxide, Cu(OH)2. *Acta Crystallogr. C* **1990,** *46*, 2279-2284
33. Wells, A. F. Malachite: re-examination of crystal structure. *Acta Crystallogr.* **1951,** *4*, (3), 200-204.
34. Eby, R. K.; Hawthorne, F. C. Cornetite: Modulated densely-packed Cu2+ oxysalt. *Miner. Petrol.* **1989,** *40*, (2), 127-136.
35. Hafner, S. S.; Nagel, S. The Electric Field Gradient at the Position of Copper in Cu2O and Electronic Charge Density Analysis by Means of K-Factors. *Phys. Chem. Miner.* **1983,** *9*, 19-22.
36. Legros, S.; Doelsch, E.; Masion, A.; Rose, J.; Borschneck, D.; Proux, O.; Hazemann, J. L.; Saint-Macary, H.; Bottero, J. Y. Combining size fractionation, scanning electron microscopy, and X-ray absorption spectroscopy to probe zinc speciation in pig slurry. *J. Environ. Qual.* **2010,** *39*, (2), 531-540.